Mon. Not. R. Astron. Soc. **000**, 000–000 (0000) Printed 13 December 2018 (MN LATEX style file v1.4)

Large Scale structure in the HI Parkes ALL-Sky Survey (HIPASS)

S. Basilakos, K. Kovač, M. Aragon, R. van de Weygaert, J. M. van der Hulst
Kapteyn Astronomical Institute, University of Groningen, The Netherlands

13 December 2018

ABSTRACT

We study the clustering properties of the recently compiled HIPASS neutral hydrogen (HI) sources catalogue using the two point correlation function in redshift space. If the two point correlation is modelled as a power law, $\xi(r) = (r_0/r)^{\gamma}$, then the best-fitting parameters for the HI selected galaxies are $r_0 = 4.3 \pm 0.3\ h^{-1}$ Mpc with $\gamma = 1.42 \pm 0.14$. Fixing the slope to its universal value $\gamma = 1.8$, we obtain $r_0 = 4.1^{+0.2}_{-0.3}\ h^{-1}$ Mpc.

Comparing the measured two point correlation function with the predictions of the concordance cosmological model ($\Omega_\Lambda = 0.7$), we find that at the present epoch the HI selected galaxies are anti-biased with respect to the underline matter fluctuation field with bias value being $b_0 \simeq 0.63$. Also, we investigate the evolution of the linear bias factor, $b(z)$, and we find to be a strongly dependent function of redshift. Finally, we estimate the HI selected galaxies redshift space distortion parameter $\beta \simeq \Omega_{\rm m}^{0.6}/b_0$ in order to correct the correlation function for the peculiar motions and we find $\beta \simeq 0.77$. Taking into account the corrections for the redshift space distortions the HI correlation length in real space is $r_0^{\rm re} = 3^{+0.4}_{-0.3} h^{-1}$Mpc for $\gamma = 1.42$ while using $\gamma = 1.8$ we get $r_0^{\rm re} = 3.1 \pm 0.3 h^{-1}$Mpc.

Keywords: galaxies: clustering - HI sources - cosmology: theory - large-scale structure of universe

1 INTRODUCTION

Over the last decades, it is well known that the clustering of the different extragalactic sources is an ideal tool for testing theories of structure formation as well as studying large-scale structure (Peebles 1993). The traditional indicator of clustering, the two-point correlation function, is a fundamental statistical test for the study of the extragalactic distribution and is relatively straightforward to measure from observational data. Recently the new generation redshift surveys such as the Point Source Catalogue for Redshift (PSC-z; Saunders et al. 2000), the European Large-Area *ISO* survey (ELAIS; Oliver et al. 2000), the Sloan Digital Sky Survey (SDSS; York et al. 2000) and the 2dF Galaxy Redshift Survey (2dFGRS; Colless et al. 2001) have extended the clustering studies and now we are able to provide with definitive measurements of galaxy clustering in the local Universe.

From a cosmological point of view, a serious issue here is how the galaxies (using different kind of data) trace the underlying mass distribution. It is well known that the large scale clustering pattern of different mass tracers (galaxies, clusters, etc) is characterised by a bias picture (Kaiser 1984). In particular, biasing is assumed to be statistical in nature; galaxies and clusters are identified as high peaks of an underlying, initially Gaussian, random density field. Biasing of galaxies with respect to the dark matter distribution was also found to be an essential ingredient of Cold Dark Matter (CDM) models of galaxy formation in order to reproduce the observed galaxy distribution (Benson et al. 2000).

In this paper we utilise the recently completed HI Parkes ALL-Sky Survey (HIPASS; Barnes et al. 2001), in which is the largest uniform and complete sample of HI selected galaxies in the local Universe, attempting to make a detailed investigation of the connection between the clustering and biasing properties of the HI selected galaxies in the framework of the concordance ΛCDM cosmology. In particular, we demonstrate the relative HI bias at the present time by comparing the observational clustering results with that derived from the concordance ($\Omega_\Lambda = 0.7$) cosmological model and describe the corresponding bias as a function of redshift. For a detailed study of the observational clustering properties of the HI sources we refer the reader to the recent work of Ryan-Weber (2006).

The structure of the paper is as follows. The observed dataset and its measured correlation function are presented in section 2. In section 3 we give a brief account of the method used to estimate the predicted correlation function in the concordance ΛCDM model,

while in section 4 we fit the HIPASS clustering to different biasing models. Finally, we draw our conclusions in section 5.

2 ESTIMATION OF THE HI SELECTED GALAXIES CORRELATION FUNCTION

2.1 The HIPASS data

In this paper we use the recent HIPASS catalogue (for more details see Meyer et al. 2004; Ryan-Weber 2006), which contains 4315 neutral hydrogen (HI) sources in the southern region of the survey $\delta < +2^{\circ}$ from 300 Km s^{-1} to 12700 Km s^{-1} and covering an area of $\sim 2.07\pi$ in the sky (see also Doyle et al. 2005). However, we are excluding detections in which the expected completeness is very low ($C < 0.5$) in order to avoid problems with the space density (estimation of the completeness limit C is given in Zwaan et al. 2004; 2005). Doing so, the remain sample contains $\sim$ 4008 HI selected galaxies with the corresponding masses being $M_{\rm HI} \leq 3\times 10^9 h^{-1} M_{\odot}$. Also it should be noted, that we describe the measured velocities in the Local Group frame and then to derive the corresponding redshifts. Therefore, redshifts are converted to proper distances using a spatially flat cosmology with $H_0 = 100h\,{\rm Km\,s^{-1}\,Mpc^{-1}}$ and $\Omega_{\rm m} = 1 - \Omega_{\Lambda} = 0.3$.

In Fig. 1, we present the estimated (histogram) and the expected for a volume limited sample (dashed line), number of the HI sources as a function of distance. It is evident that the number of HI sources appears to follow the equal-volume law out to $11.5h^{-1}$Mpc, a fact corroborated also from the standard Kolmogorov-Smirnov (KS) test which gives probability of consistency between model and observations (up to $r \leq 10h^{-1}$Mpc) of $\mathcal{P}_{\rm KS} \simeq 0.40$. However, due to the fact that the HIPASS catalogoue is a peak flux limited sample there is the well known degradation of sampling as a function of distance (codified by the so called *selection function*). Thus, we can attempt to parametrise our results for this particular effect using the following formula:

$$\frac{{\rm d}N}{{\rm d}r} = Ar^{2+\alpha}\exp\left[-(r/r_s)^m\right] \quad (1)$$

with

$$A = \frac{Nm}{\Gamma(\frac{\alpha+3}{m})r_s^{\alpha+3}} \quad (2)$$

where N is the total number of the HI sources and the factor Γ is the Γ function. The line corresponds to the best-fitting dN/dr, which is determined by the standard χ^2 minimisation procedure in which each part of the histogram is weighted by its Poisson error^{-1}. The reduced χ^2/dof is ~ 0.90 and the corresponding values fitted parameters are $r_s = 16.5^{+1.0}_{-2.5}h^{-1}$Mpc, $m = 1.24^{+0.06}_{-0.08}$ and $\alpha = -0.30 \pm 0.12$ (within 1σ errors). To this end in Fig. 2 we show the number density of our sample as a function of distance. It is obvious that up to $\sim 11.5h^{-1}$Mpc the corresponding density remains almost the same and then drops because of the selection function. Therefore, it becomes obvious that the mean density of the HIPASS sample is $< \rho > \simeq 0.14h^3\,{\rm Mpc}^{-3}$.

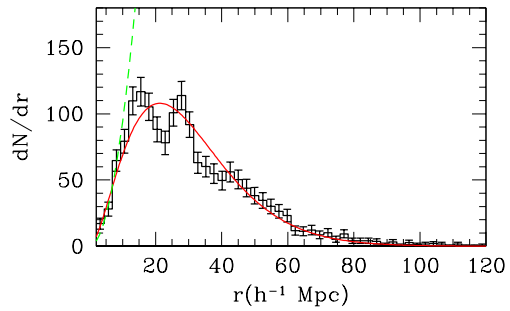

Figure 1. The measured (histogram) and the fitted (line) number of the HI sources as a function of distance. The dashed line corresponds to a volume limited sample.

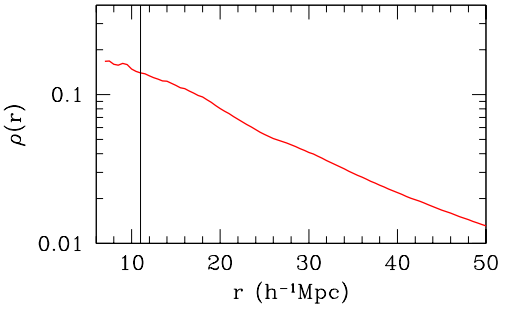

Figure 2. The number density of the HIPASS data as a function of distance.

2.2 HI selected galaxy correlations

In this paper we will present for the first time a study of the clustering ⋆ and biasing properties of the HI 21-cm emission line sources from HIPASS catalogue. In particular, we estimate the redshift space correlation function using the estimator described by Hamilton (1993):

$$\xi(r) = 4\frac{N_{DD}\langle N_{RR}\rangle}{\langle N_{DR}\rangle^2} - 1 \quad (3)$$

where N_{DD} is the number of HI pairs in the interval $[r-\Delta r, r+\Delta r]$. While, $\langle N_{RR}\rangle$ and $\langle N_{DR}\rangle$ is the average, over 100 random simulations with the same properties as the real data (boundaries, completeness and selection function), HI-random and random-random pairs, respectively. In fact the random catalogues were constructed by randomly reshuffling the angular coordinates of the HI sources (within the limits of the catalogue), while keeping the same distance and thus exactly the same selection function as the real data. The latter indeed is essential in order to take into account the possible systematic effects (eg. completeness, fraction of HI sources missed by the finding algorithm due

⋆ For the HI clustering see also Ryan-Weber (2006).

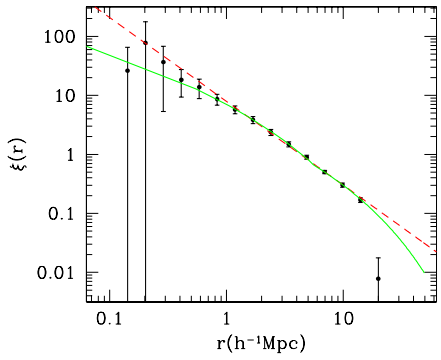

Figure 3. The spatial two-point correlation function (points) in redshift space for HIPASS sample. The error bars are estimated using the bootstrap procedure. The dashed line represent the best-fitting power low $\xi(r) = (r_0/r)^{\gamma}$ (see parameters in Table 1), while the continuous line represents the best fit ΛCDM ($\Omega_{\Lambda} = 0.7$ and $h = 0.7$) model in the framework of $b_0 = 0.63$.

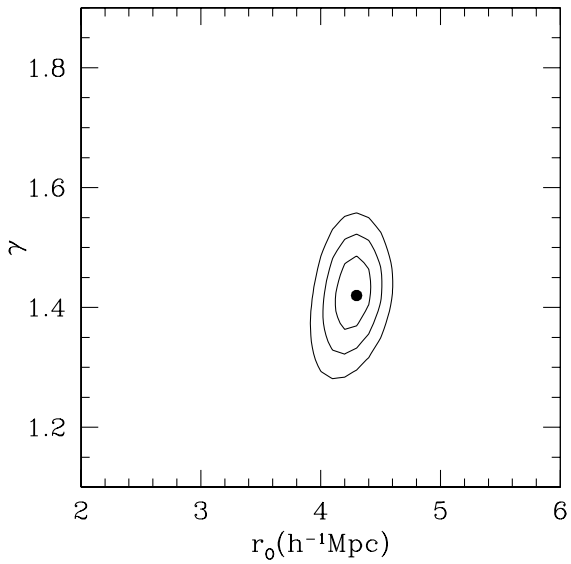

Figure 4. Iso-$\Delta\chi^2$ contours in the $r_0 - \gamma$ parameter space for the HIPASS sample. (continuous line) and S_2 (dashed line) samples. The contours correspond to 1σ ($\Delta\chi^2 = 2.30$), 2σ ($\Delta\chi^2 = 6.17$) and 3σ ($\Delta\chi^2 = 11.8$) uncertainties.

to the HIPASS flux limit). Note that we compute the errors on $\xi(r)$ from 100 bootstrap re-samplings of the data (Mo, Jing & Börner 1992).

Furthermore, we apply the correlation analysis to the HIPASS sample evaluating $\xi(r)$ in logarithmic intervals. In Fig. 3, we present the estimated two point redshift correlation function (dots); clustering is evident. We see that the correlation function below $r \geq 11h^{-1}$Mpc drops dramatically. The dashed line corresponds to the best-fitting power law model $\xi(r) = (r_0/r)^{\gamma}$, which is determined by the standard χ^2 minimisation procedure in which each correlation point is weighted by its error^{-1}. In Fig. 4 we present the iso-$\Delta\chi^2$ contours (where $\Delta\chi^2 = \chi^2 - \chi^2_{\rm min}$) in the $r_0 - \gamma$ plane. The $\chi^2_{\rm min}$ is the absolute minimum value of the χ^2. The contours correspond to 1σ ($\Delta\chi^2 = 2.30$), 2σ ($\Delta\chi^2 = 6.17$) and 3σ ($\Delta\chi^2 = 11.8$) uncertainties, respectively. The best fit parameters are listed in Table 1. Note that, the fit has been performed taking into account bins with $r \geq 0.5$ h^{-1}Mpc in order to avoid the signal from very small and therefore highly non-linear scales, while we have used no upper r cut-off (our results remain robust by varying the upper r limit within the 5 to 20 h^{-1} Mpc range).

Therefore, the clustering parameters are $r_0 = 4.3 \pm 0.3h^{-1}$Mpc and $\gamma = 1.42 \pm 0.14$. Fixing now the correlation function slope to its nominal value of $\gamma = 1.8$ we found $r_0 = 4.1^{+0.2}_{-0.3}h^{-1}$Mpc but the fit is good for $r > 1h^{-1}$Mpc. Our results is in relatively good agreement with those derived by Ryan-Weber (2006), $r_0 = 3.1 \pm 0.5h^{-1}$Mpc and $\gamma = 1.4 \pm 0.5$ using the HIPASS data. Also, in the local Universe, our results can be compared with those found by the following papers: (a) Zehavi et al. (2002) and Hawkins et al. (2003), $r_0 \simeq 5h^{-1}$Mpc and $\gamma \simeq 1.7$ for the SDSS galaxies (b) Norberg et al. (2001), $r_0 \simeq 4.9h^{-1}$Mpc and $\gamma \simeq 1.7$ for the 2dFGRS galaxies, (c) Jing, Börner & Suto (2002), $r_0 \simeq 3.7h^{-1}$Mpc and $\gamma \simeq 1.7$ using the PSCz data and finally Gonzalez-Solares et al. (2004), $r_0 \simeq 4.3h^{-1}$Mpc and $\gamma \simeq 2$ using the ELAIS sources. † However, it should point out that these authors found a somewhat greater slope for the correlation function.

3 MODEL HI SELECTED GALAXY CORRELATIONS

It is well known (cf. Kaiser 1984; Benson et al. 2000) that according to linear biasing the correlation function of the mass-tracer ($\xi_{\rm obj}$) and dark-matter one ($\xi_{\rm DM}$), are related by:

$$\xi_{\rm obj}(r) = b_0^2 \xi_{\rm DM}(r) \ , \qquad (4)$$

where b_0 is the bias factor at the present time. We quantify the underlying matter distribution clustering by presenting the spatial correlation function of the mass $\xi_{\rm DM}(r)$ [in general this is a function of redshift] as the Fourier transform of the spatial power spectrum $P(k)$:

$$\xi_{\rm DM}(r) = \frac{1}{2\pi^2} \int_0^{\infty} k^2 P(k) \frac{\sin(kr)}{kr} {\rm d}k \ , \qquad (5)$$

where k is the comoving wavenumber.

As for the power spectrum, we consider that of CDM models, where $P(k) \approx k^n T^2(k)$ with scale-invariant ($n = 1$) primeval inflationary fluctuations. We utilise the transfer function parameterisation as in Bardeen et al. (1986), with the approximate corrections given by Sugiyama's (1995) formula:

† The robustness of our results to the fitting procedure was tested using different bins (spanning from 10 to 20) and we found very similar clustering results.

Table 1. Results of the correlation function analysis for HI selected galaxies of the HIPASS sample. Errors of the fitted parameters represent 3σ uncertainties. Finally, the r_0 has units of h^{-1} Mpc.

r_0	γ	$r_0(\gamma=1.8)$	b_0	β	$K(\beta)$	$r_0^{\rm re}$	$r_0^{\rm re}(\gamma=1.8)$
4.3 ± 0.3	1.42 ± 0.14	$4.1^{+0.2}_{-0.3}$	0.63 ± 0.03	0.77	1.63	3.1 ± 0.3	$3^{+0.4}_{-0.3}$

$$T(k)=\frac{\ln(1+2.34q)}{2.34q}[1+3.89q+(16.1q)^2+$$

$$(5.46q)^3+(6.71q)^4]^{-1/4} \quad .$$

with

$$q=\frac{k}{\Omega_{\rm m}h^2{\rm exp}[-\Omega_b-(2h)^{1/2}\Omega_b/\Omega_{\rm m}]} \qquad (6)$$

where $k=2\pi/\lambda$ is the wavenumber in units of h Mpc^{-1} and Ω_b is the baryon density. Note that we also use the non-linear corrections introduced by Peacock & Dodds (1994).

In the present analysis we consider the concordance model ($\Omega_{\rm m}=0.3$) with cosmological parameters that fit the majority of observations, ie., $\Omega_{\rm m}+\Omega_\Lambda=1$, $H_0=100h$km s^{-1} Mpc^{-1} with $h\simeq0.7$ (cf. Freedman et al. 2001; Peebles and Ratra 2003; Spergel et al. 2003; Tonry et al. 2003; Riess et al. 2004; Tegmark et al. 2004; Basilakos & Plionis 2005 and references therein), baryonic density parameter $\Omega_{\rm b}h^2\simeq0.02$ (e.g. Olive, Steigman & Walker 2000; Kirkman et al 2003) and a CDM shape parameter $\Gamma=0.17$. Note that all the concordance model is normalised to have fluctuation amplitude, in a sphere of 8 h^{-1}Mpc radius, of $\sigma_8\simeq0.50(\pm0.1)\Omega_{\rm m}^{-0.53}$ (the general formula provided by Wang & Steinhardt 1998).

4 THE HIPASS BIASING

In order to quantify the HIPASS bias at the present time we perform a standard χ^2 minimisation procedure (described before) between the measured correlation function of the HIPASS sources with that expected in the concordance model

$$\chi^2(b_0)=\sum_{i=1}^{n}\left[\frac{\xi^i(r)-\xi^i_{\rm obj}(r,b_0)}{\sigma^i}\right]^2 \quad , \qquad (7)$$

where σ^i is the observed correlation function (bootstrap) uncertainty.

Doing so the bias factor at the present time is $b_0=0.63\pm0.03$. Note, that from a theoretical point of view it is well known that the bias parameter for the present day halos with $M\leq10^{12}h^{-1}M_\odot$ is $\simeq0.65$ (Sheth, Mo & Tormen 2001; Jing 1999; Seljak & Warren 2004). Thus it seems, that in the local Universe the HI selected galaxies are anti-biased tracers of the underlying matter distribution. This is to be expected, simply because our clustering analysis produces a lower corresponding correlation length (see Table 1) than the nominal one ($\sim5.5h^{-1}$Mpc). In other words, the higher or lower correlation length corresponds to a higher or lower bias at the present time respectively, being consistent with the hierarchical clustering scenario (cf. Magliocchetti et al. 2000 and references therein).

To this end, owing to the fact that the observational data are analysed in redshift space, the correlations should be amplified by the factor $K(\beta)=1+2\beta/3+\beta^2/5$ (Hamilton 1992, also see Hawkins et al. 2003) in the linear regime, where $\beta\simeq\Omega_{\rm m}^{0.6}/b_0$. Also in Table 1 we list the results of the fits for our HIPASS data, ie., the value of the HI optical bias, b_0, at the present time, as well as the redshift distortion β parameter and a measure of the $K(\beta)$ correction. Multiplying with $K^{-1}(\beta)$ to each bin of our redshift space correlation function $\xi(r)$ and repeating the fitting (see the last two columns of Table 1) the correlation length in real space is $r_0^{\rm re}=3^{+0.4}_{-0.3}h^{-1}$Mpc for $\gamma=1.42$ while using $\gamma=1.8$ we get $r_0^{\rm re}=3.1\pm0.3h^{-1}$Mpc. Finally, in Fig. 3, we plot the measured $\xi(r)$ of the HIPASS sample with the estimated (continuous line) two point correlation function for the concordance model using $b_0=0.63$. It is obvious that the fit works extremely well.

4.1 Morphological Properties

The above statistical approach (low biasing at the present epoch) introduces that there is a strong indication that the HI sources could relatively trace low density regimes of the underlying matter distribution (see also Grogin & Geller 1998). In order to investigate that, in Fig.5 we present a three dimensional view of the HIPASS data after using a novel technique which is based on the Multiscale Morphology Filters (Aragon et al. 2006 in preparation). Note that the dark and the light grey configurations correspond to filament-like structures and clusters of HI galaxies respectively. More than half of the HIPASS galaxies ($\sim55\%$) belong to morphologicaly undefined regions of the 3D distribution which are related to low density regions. This is simply to be expected because of the low biasing ($b_0\simeq0.63$). The rest of the objects are estimated to be in clusters ($\sim18\%$, light grey structures) and superclusters ($\sim27\%$, dark grey structures).

4.2 Bias Evolution

In order to understand better the effects of HI clustering, in this section we investigate the HI bias factor as a function of redshift. From a cosmological point of view, the evolution of neutral hydrogen is a powerful tool of tracing structure formation as a function of redshift because it indicates the rate of evolution of gas into stars and thus the gas consumption and the amount of the star formation in the Universe.

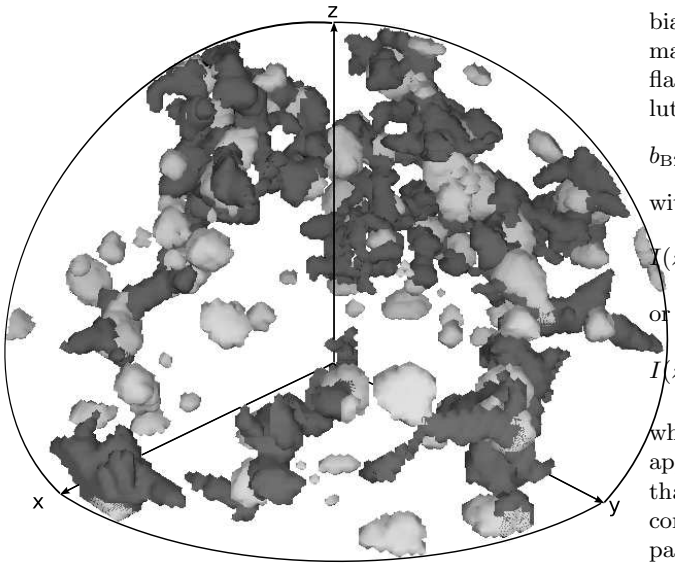

Figure 5. The 3D distribution of the HI selected galaxies in the local Universe (based on the Multiscale Morphology Filters). Note that the dark and the light grey structures correspond to superclusters and clusters of HIPASS galaxies respectively.

Over the past two decades, based on different assumptions, a number of bias evolution models have been proposed (eg. Nusser & Davis 1994; Fry 1996; Mo & White 1996; Matarrese et al. 1997; Tegmark & Peebles 1998; Basilakos & Plionis 2001). However, here we will discuss models that have been shown to describe relatively well the evolution even beyond $z \sim 1$.

• *Merging Bias Model* (hereafter B1): Mo & White (1996) have developed a model for the evolution of the the so-called correlation bias, using the Press-Schechter formalism. Utiling a similar formalism, Matarrese et al. (1997) extended the Mo & White (1996) results to include the effects of different mass scales (see also Bagla 1998). In this case the expression which describes the bias evolution is

$$b_{\rm B2}(z) = 0.41 + \frac{(b_0 - 0.41)}{D^{\beta}(z)} \quad , \tag{8}$$

with $\beta \simeq 1.8$. Note that $D(z)$ is the linear growth rate of clustering (cf. Peebles 1993) ‡ scaled to unity at the present time.

$$D(z) = \frac{5\Omega_{\rm m} E(z)}{2} \int_z^{\infty} \frac{(1+x)}{E^3(x)} {\rm d}x \ . \tag{9}$$

with

$$E(z) = \left[\Omega_{\rm m}(1+z)^3 + \Omega_{\Lambda}\right]^{1/2} \ . \tag{10}$$

• *Bias from Linear Perturbation Theory* (hereafter B2): Basilakos & Plionis (2001, 2003), using linear perturbation theory and the Friedmann-Lemaitre solutions of the cosmological field equations have derived analytically the functional form for the evolution of the linear bias factor, b, between the background matter and a mass-tracer fluctuation field. For the case of a spatially flat Λ cosmological model ($\Omega_{\rm m} + \Omega_{\Lambda} = 1$), the bias evolution can be written as:

$$b_{\rm B2}(z) = \mathcal{C}_1 E(z) + \mathcal{C}_2 E(z) I(z) + 1 \tag{11}$$

with

$$I(z) = \int_{1+z}^{\infty} \frac{y^3}{[\Omega_{\rm m} y^3 + \Omega_{\Lambda}]^{3/2}} {\rm d}y \tag{12}$$

or

$$I(z) = (1+z)^{-1/2} F\left[\frac{1}{6}, \frac{3}{2}, \frac{7}{6}, -\frac{\Omega_{\Lambda}}{\Omega_{\rm m}(1+z)^3}\right] \tag{13}$$

where F is the hyper-geometric function. Note that this approach gives a family of bias curves, due to the fact that it has two unknown parameters, (the integration constants $\mathcal{C}_1, \mathcal{C}_2$). Basilakos & Plionis (2001, 2003) compared the B2 bias evolution model with other models as well as with the HDF (Hubble Deep Field) biasing results (Arnouts et al. 2002), and found a very good consistency. Of course in order to obtain partial solutions for $b(z)$ we need to estimate the values of the constants $\mathcal{C}_1$ and $\mathcal{C}_2$), which means that we need to calibrate the $b(z)$ relation using two different epochs: $b(0) = b_0$ and $b(z_1) = b_1$.

Therefore, utilised the general bias solution (see eq.11), it is routine to obtain the expressions for the above constants as a function of b_0 and b_1:

$$\mathcal{C}_1 = \frac{(b_0 - 1)E(z_1)I(z_1) - (b_1 - 1)E(0)I(0)}{E(0)E(z_1)[I(z_1) - I(0)]} \tag{14}$$

$$\mathcal{C}_2 = \frac{E(0)(b_1 - 1) - E(z_1)(b_0 - 1)}{E(0)E(z_1)[I(z_1) - I(0)]} \quad , \tag{15}$$

where for the present epoch we have: $b_0 \simeq 0.63$, $E(0) = 1$ and $I(0) \simeq 9.567$. In the distant Universe we calibrate the B2-model by using Cooke et al. (2006) value of the bias for Damped Lyman-a systems (hereafter DLA; see solid point in Fig.6) which gives, $b(3) \simeq 2.4$ §. The DLA systems are quasar absorbers along the line-of-sight at high redshifts and they are classified according to their large column densities, $N_{\rm HI} \geq 2 \times 10^{20}$atom cm$^{-}2$ (see Wolfe et al. 1986; Peroux et al. 2001). These systems play a vital role in the hierarchy of the structure formation because the large column densities can protect large amounts of neutral gas from the background ionizing (Zwaan & Prochaska 2006) and thus they produce an ideal environment for star formation.

Having known the bias factor at the present time in Fig.6 we plot the quantity $b(z)$ as a function of redshift for the concordance cosmological model and for different bias evolution models (B1 continuous line and B2 dashed line). It is quite obvious that the behaviour of the function $b(z)$ characterises the tracing evolution with epoch; in particular at low redshifts ($z \leq 0.9$) we have a sort of anti-bias picture but latter on owing to the fact that the bias is a monotonically increasing function of redshift for both B1 and B2 biasing models the HI

‡ $D(z) = (1+z)^{-1}$ for an Einstein-de Sitter Universe.

§ For $z = 3$ we get $E(3) \simeq 4.61$ and $I(3) \simeq 6.039$

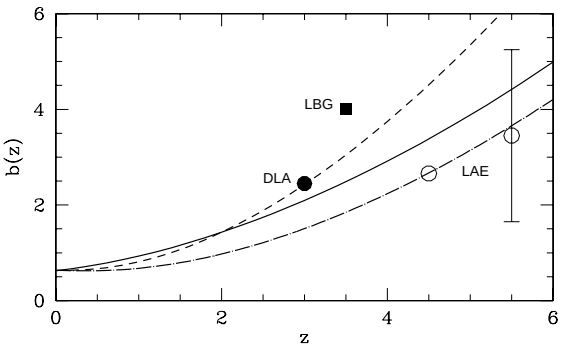

Figure 6. The bias factor as a function of redshift for the B1 (continuous line) and B2 (dashed line) bias model respectively. Different point types represent different values of bias. The solid circle represents the observational bias for the Damped Lyman-a systems (DLA) of Cooke et al. (2006). The square like symbol corresponds to Lyman break galaxies (LBG, Steidel et al. 1998) while the open circle represents the bias for the Lyman-a emitters (LAE) derived by Ouchi et al. (2005) and Kovač et al. (in preparation). Note that the dot-dashed line represents the bias behavior for the LAE galaxies.

sources are biased with respect to the underlying matter distribution. Also up to redshift 2.2 both models give almost the same predictions. However, at very high redshifts Fig.6 clearly shows that the bias of those neutral hydrogen sources behaves different in the different biasing models.

We further compare our analytic solutions with observations provided by (a) Steidel et al. (1998) which confirmed that the Lyman-break galaxies (hereafter LBG; see solid square in Fig.6) are very strongly biased tracers of mass (see also Adelberger et al. 1998; Kashikawa et al. 2006) and they found that $b(3.4) \simeq 4$ and (b) Ouchi et al. (2005) utilising Lyman-a emitters found $b(5.7) \simeq 3.8 \pm 1.8$ while Kovač et al (in preparation) found $b(4.5) = 2.6$ (hereafter LAE; see open circle in Fig.6). In that case, we compare in Fig.6 (dot dashed line) the B2-model, evaluated at $z = 4.5$ ¶ using the LAE results (Kovač et al. in preparation). It is quite evident that our model fits better the z-dependance of the observational LAE galaxy bias. Our strong biasing predictions are also in agreement with those found from simulations of galaxy formation (Kauffmann et al. 1999) which means that such strong biasing at large redshifts can be justified if structures are formed at the highest rare peaks of matter density (Mo & White 2002). From the observational point of view the last few years many authors using Lyman-a systems have found high overdensities ($\delta > 50$) at high redshifts. Indeed, Steidel et al. (1998) using LBGs found a very high overdensity peak (protocluster) at $z = 3.1$. Recently, Venemans et al. (2004), Miley et al. (2004) and Ouchi et al. (2005) found protoclusters of LAE galaxies at high redshifts ($z \geq 4$). Also cross correlation analysis has shown (Cooke et al. 2006) that the LBGs associated with the DLA systems at the same redshift a fact which implies that perhaps the LBGs are in the same parent system that contains DLAs (Cooke et al. 2005).

¶ For $z = 4.5$ we get $E(4.5) \simeq 7.11$ and $I(4.5) \simeq 5.175$

5 CONCLUSIONS

We have studied the clustering properties of the HI 21-cm emission line sources from HIPASS catalogue in redshift space. We find that if the two point cluster correlation function is modelled as a power law, $\xi(r) = (r_0/r)^{\gamma}$, then the best-fitting parameters are $r_0 = 4.3 \pm 0.3h^{-1}$ Mpc with $\gamma = 1.42 \pm 0.14$. Fixing the slope to its universal value $\gamma = 1.8$, we obtain $r_0 = 4.1^{+0.2}_{-0.3}h^{-1}$Mpc.

Comparing the measured spatial correlation function for the HI selected galaxies with the theoretical predictions of the preferred ΛCDM cosmological model ($\Omega_{\rm m} = 1 - \Omega_{\Lambda} = 0.3$) and two different bias evolution models, we find that the present bias value is $b_0 \simeq 0.63$, suggesting that the HI selected galaxies could potentially trace the low density regimes in the local Universe in agreement with previous studies (Grogin & Geller 1998). Also, we investigate the evolution of the linear bias factor, $b(z)$, and we find that the anti-bias behaviour extends up to $z \leq 0.9$. Our predictions are consistent with the observational bias results of the Lyman-a galaxies. Furthermore, we estimate the HIPASS redshift space distortion parameter $\beta \simeq 0.77$ and we conclude that the amplitude of the HI redshift correlation function increases by a factor of 1.63. Therefore, taking into account this correction the HI correlation length in real space is $r_0^{\rm re} = 3^{+0.4}_{-0.3}h^{-1}$Mpc for $\gamma = 1.42$ while using $\gamma = 1.8$ we get $r_0^{\rm re} = 3.1 \pm 0.3h^{-1}$Mpc.

ACKNOWLEDGEMENTS

SB acknowledges support by the Nederlandse Onderzoekschool voor Astronomie (NOVA) grant No 366243.

REFERENCES

Adelberger, K. L., Steidel, C. C., Giavalisko, M., Dickinson M., Pettini, M., &, Kellogg, M., 1998, ApJ, 505, 18
Arnouts, S., et al.., 2002, MNRAS, 329, 355
Bagla, J. S., 1998, MNRAS, 299, 424
Barnes et al., 2001, MNRAS, 322, 486
Bardeen, J.M., Bond, J.R., Kaiser, N. & Szalay, A.S., 1986, ApJ, 304, 15
Basilakos, S. & Plionis, M., 2001, ApJ, 550, 522
Basilakos, S. & Plionis, M., 2003, ApJ, 593, L61
Basilakos, S. & Plionis, M., 2005, MNRAS, 360, L35
Benson A. J., Cole S., Frenk S. C., Baugh M. C., & Lacey G. C., 2000, MNRAS, 311, 793
Colless, M., et al., 2001, MNRAS, 328, 1039
Cooke, J. W., Wolfe, A. M., Prochaska, J. X.,&, Gawiser, E., 2005, ApJ, 621, 596
Cooke, J. W., Wolfe, A. M., Gawiser, E., &, Prochaska, J. X., 2006, ApJ, 636, L9
Doyle, M. T., et al., 2005, MNRAS, 361, 34

Freedman, W., L., et al., 2001, ApJ, 553, 47
Fry J.N., 1996, ApJ, 461, 65
Gonzalez-Solares, E. A., et al., MNRAS, 352, 44
Grogin, N. A., &, Geller, M. J., 1998, ApJ, 505, 506
Jing, Y. P., 1999, ApJ, 515, 45
Jing, Y. P., Börner, G & Suto, Y., 2002, ApJ, 564, 15
Hamilton, A. J. S., 1992, ApJ, 385, L5
Hamilton, A. J. S., 1993, ApJ, 417, 19
Hawkins, Ed, et al., 2003, MNRAS, 346, 78
Kaiser N., 1984, ApJ, 284, L9
Kashikawa, N., et al., 2006, ApJ, 637, 631
Kauffmann G., Golberg, J. M., Diaferio A., &, White S. D. M., 1999, MNRAS, 307, 529
Kirkman, D., Tytler, D., Suzuki, N., O'Meara, J.M. & Lubin, D., 2003, ApJS, 149, 1
Magliocchetti, M., Bagla, J. S., Maddox, S. J. & Lahav, O., 2000, MNRAS, 314,546
Mataresse, S., Coles, P., Lucchin, F. & Moscardini, L., 1997, MNRAS, 286, 115
Meyer, G. R., et al., 2004, MNRAS, 350, 1195
Miley, G. K.., et al., 2004, Nature, 427, 47
Mo, H. J., Jing, Y. P. & Börner, G., 1992, ApJ, 392, 452
Mo, H.J, & White, S.D.M 1996, MNRAS, 282, 347
Mo, H.J, & White, S.D.M 2002, MNRAS, 336, 112
Norberg, P., et al., 2001, MNRAS, 328, 64
Nusser, M., & Davis, M., 1994, ApJ, 421, L1
Olive, K.A., Steigman, G. & Walker, T.P., 2000, Phys.Rep., 333, 389
Oliver, S., et al., 2000, MNRAS, 316, 749
Ouchi, M., et al., 2005, ApJ, 620, l10
Peacock, A. J., &, Dodds, S. J., 1994, MNRAS, 267, 1020
Peebles P.J.E., 1993, Principles of Physical Cosmology, Princeton University Press, Princeton New Jersey
Peebles P.J.E., &, Ratra, B., 2003, RvMP, 75, 559
Peroux, C., Storrie-Lombardi, L. J., McMahon, R. G., Irwin, M., &, Hook, I. M., 2001, AJ, 121, 1799
Riess, A. G., et al., 2004, ApJ, 607, 665
Ryan-Weber, E. V., MNRAS, 2006, in press, *astro-ph/0601055*
Saunders, W., et al., 2000, MNRAS, 317, 55
Seljak U., &, Warren, M. S., 2004, MNRAS, 355, 129
Sheth R. K., Mo H. J., &, Tormen, G., 2001, MNRAS, 323, 1
Spergel, D. N., et al., 2003, ApJs, 148, 175
Steidel C.C., Adelberger L.K., Dickinson M., Giavalisko M., Pettini M., &, Kellogg M., 1998, ApJ, 492, 428
Sugiyama, N., 1995, ApJS, 100, 281
Tegmark M. & Peebles P.J.E, 1998, ApJL, 500, L79
Tegmark M., et al., 2004, Phys. Rev. D., 69, 3501
Tonry, et al. , 2003, ApJ, 594, 1
Wang, L. & Steinhardt, P.J., 1998, ApJ, 508, 483
Wolfe, A. M., Tumshek, D. A., Smith, H. E., &, Cohen, R. D., 1986, ApJS, 61, 249
Venemans, B. P., et al., 2004, A&A, 427, L17
York, D. G., 2000, AJ, 120, 1579
Zehavi I., et al., 2002, ApJ, 571, 172
Zwaan, M. A., et al., 2004, MNRAS, 350, 1210
Zwaan, M. A., Meyer, M. J., Staveley-Smith, L., Webster, R. L., 2005, MNRAS, 359, L30
Zwaan, M. A., &, Prochaska, J. X., 2006, ApJ, in press, *astro-ph/0601655*

Mon. Not. R. Astron. Soc. **000**, 000–000 (0000) Printed 3 February 2006 (MN LATEX style file v1.4)

Large Scale structure in the HI Parkes ALL-Sky Survey (HIPASS)

S. Basilakos, K. Kovač, M. Aragon, R. van de Weygaert, J. M. van der Hulst
Kapteyn Astronomical Institute, University of Groningen, The Netherlands

3 February 2006

ABSTRACT
We study the clustering properties of the recently compiled HIPASS neutral hydrogen (HI) sources catalogue using the two point correlation function in redshift space. If the two point correlation is modelled as a power law, $\xi(r) = (r_0/r)^\gamma$, then the best-fitting parameters for the HI selected galaxies are $r_0 = 4.3 \pm 0.3\, h^{-1}$ Mpc with $\gamma = 1.42 \pm 0.14$. Fixing the slope to its universal value $\gamma = 1.8$, we obtain $r_0 = 4.1^{+0.2}_{-0.3}\, h^{-1}$ Mpc.

Comparing the measured two point correlation function with the predictions of the concordance cosmological model ($\Omega_\Lambda = 0.7$), we find that at the present epoch the HI selected galaxies are anti-biased with respect to the underline matter fluctuation field with bias value being $b_0 \simeq 0.63$. Also, we investigate the evolution of the linear bias factor, $b(z)$, and we find to be a strongly dependent function of redshift. Finally, we estimate the HI selected galaxies redshift space distortion parameter $\beta \simeq \Omega_{\rm m}^{0.6}/b_0$ in order to correct the correlation function for the peculiar motions and we find $\beta \simeq 0.77$. Taking into account the corrections for the redshift space distortions the HI correlation length in real space is $r_0^{\rm re} = 3^{+0.4}_{-0.3} h^{-1}$Mpc for $\gamma = 1.42$ while using $\gamma = 1.8$ we get $r_0^{\rm re} = 3.1 \pm 0.3 h^{-1}$Mpc.

Keywords: galaxies: clustering - HI sources - cosmology: theory - large-scale structure of universe

1 INTRODUCTION

Over the last decades, it is well known that the clustering of the different extragalactic sources is an ideal tool for testing theories of structure formation as well as studying large-scale structure (Peebles 1993). The traditional indicator of clustering, the two-point correlation function, is a fundamental statistical test for the study of the extragalactic distribution and is relatively straightforward to measure from observational data. Recently the new generation redshift surveys such as the Point Source Catalogue for Redshift (PSC-z; Saunders et al. 2000), the European Large-Area *ISO* survey (ELAIS; Oliver et al. 2000), the Sloan Digital Sky Survey (SDSS; York et al. 2000) and the 2dF Galaxy Redshift Survey (2dFGRS; Colless et al. 2001) have extended the clustering studies and now we are able to provide with definitive measurements of galaxy clustering in the local Universe.

From a cosmological point of view, a serious issue here is how the galaxies (using different kind of data) trace the underlying mass distribution. It is well known that the large scale clustering pattern of different mass tracers (galaxies, clusters, etc) is characterised by a bias picture (Kaiser 1984). In particular, biasing is assumed to be statistical in nature; galaxies and clusters are identified as high peaks of an underlying, initially Gaussian, random density field. Biasing of galaxies with respect to the dark matter distribution was also found to be an essential ingredient of Cold Dark Matter (CDM) models of galaxy formation in order to reproduce the observed galaxy distribution (Benson et al. 2000).

In this paper we utilise the recently completed HI Parkes ALL-Sky Survey (HIPASS; Barnes et al. 2001), in which is the largest uniform and complete sample of HI selected galaxies in the local Universe, attempting to make a detailed investigation of the connection between the clustering and biasing properties of the HI selected galaxies in the framework of the concordance ΛCDM cosmology. In particular, we demonstrate the relative HI bias at the present time by comparing the observational clustering results with that derived from the concordance ($\Omega_\Lambda = 0.7$) cosmological model and describe the corresponding bias as a function of redshift. For a detailed study of the observational clustering properties of the HI sources we refer the reader to the recent work of Ryan-Weber (2006).

The structure of the paper is as follows. The observed dataset and its measured correlation function are presented in section 2. In section 3 we give a brief account of the method used to estimate the predicted correlation function in the concordance ΛCDM model,

while in section 4 we fit the HIPASS clustering to different biasing models. Finally, we draw our conclusions in section 5.

2 ESTIMATION OF THE HI SELECTED GALAXIES CORRELATION FUNCTION

2.1 The HIPASS data

In this paper we use the recent HIPASS catalogue (for more details see Meyer et al. 2004; Ryan-Weber 2006), which contains 4315 neutral hydrogen (HI) sources in the southern region of the survey $\delta < +2^{\circ}$ from 300 Km s^{-1} to 12700 Km s^{-1} and covering an area of $\sim 2.07\pi$ in the sky (see also Doyle et al. 2005). However, we are excluding detections in which the expected completeness is very low ($C < 0.5$) in order to avoid problems with the space density (estimation of the completeness limit C is given in Zwaan et al. 2004; 2005). Doing so, the remain sample contains $\sim$ 4008 HI selected galaxies with the corresponding masses being $M_{\rm HI} \leq 3 \times 10^9 h^{-1} M_{\odot}$. Also it should be noted, that we describe the measured velocities in the Local Group frame and then to derive the corresponding redshifts. Therefore, redshifts are converted to proper distances using a spatially flat cosmology with $H_0 = 100h\,{\rm Km s^{-1}\,Mpc^{-1}}$ and $\Omega_{\rm m} = 1 - \Omega_{\Lambda} = 0.3$.

In Fig. 1, we present the estimated (histogram) and the expected for a volume limited sample (dashed line), number of the HI sources as a function of distance. It is evident that the number of HI sources appears to follow the equal-volume law out to $11.5h^{-1}$Mpc, a fact corroborated also from the standard Kolmogorov-Smirnov (KS) test which gives probability of consistency between model and observations (up to $r \leq 10h^{-1}$Mpc) of $\mathcal{P}_{\rm KS} \simeq 0.40$. However, due to the fact that the HIPASS catalogoue is a peak flux limited sample there is the well known degradation of sampling as a function of distance (codified by the so called *selection function*). Thus, we can attempt to parametrise our results for this particular effect using the following formula:

$$\frac{{\rm d}N}{{\rm d}r} = Ar^{2+\alpha} \exp\left[-(r/r_s)^m\right] \quad (1)$$

with

$$A = \frac{Nm}{\Gamma(\frac{\alpha+3}{m}) r_s^{\alpha+3}} \quad (2)$$

where N is the total number of the HI sources and the factor Γ is the Γ function. The line corresponds to the best-fitting dN/dr, which is determined by the standard χ^2 minimisation procedure in which each part of the histogram is weighted by its Poisson error^{-1}. The reduced χ^2/dof is ~ 0.90 and the corresponding values fitted parameters are $r_s = 16.5^{+1.0}_{-2.5} h^{-1}$Mpc, $m = 1.24^{+0.06}_{-0.08}$ and $\alpha = -0.30 \pm 0.12$ (within 1σ errors). To this end in Fig. 2 we show the number density of our sample as a function of distance. It is obvious that up to $\sim 11.5h^{-1}$Mpc the corresponding density remains almost the same and then drops because of the selection function. Therefore, it becomes obvious that the mean density of the HIPASS sample is $< \rho > \simeq 0.14h^3$ Mpc^{-3}.

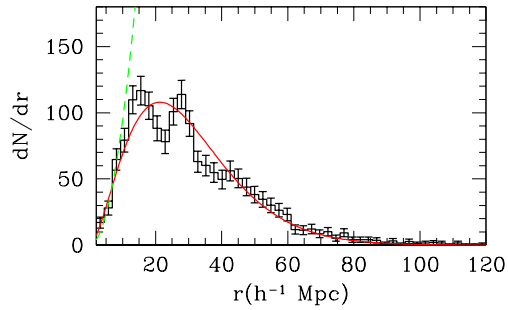

Figure 1. The measured (histogram) and the fitted (line) number of the HI sources as a function of distance. The dashed line corresponds to a volume limited sample.

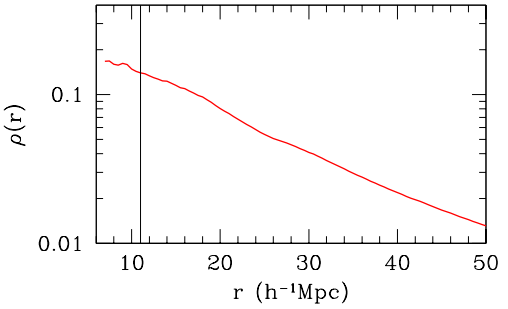

Figure 2. The number density of the HIPASS data as a function of distance.

2.2 HI selected galaxy correlations

In this paper we will present for the first time a study of the clustering ⋆ and biasing properties of the HI 21-cm emission line sources from HIPASS catalogue. In particular, we estimate the redshift space correlation function using the estimator described by Hamilton (1993):

$$\xi(r) = 4\frac{N_{DD}\langle N_{RR}\rangle}{\langle N_{DR}\rangle^2} - 1 \quad (3)$$

where N_{DD} is the number of HI pairs in the interval $[r-\Delta r, r+\Delta r]$. While, $\langle N_{RR}\rangle$ and $\langle N_{DR}\rangle$ is the average, over 100 random simulations with the same properties as the real data (boundaries, completeness and selection function), HI-random and random-random pairs, respectively. In fact the random catalogues were constructed by randomly reshuffling the angular coordinates of the HI sources (within the limits of the catalogue), while keeping the same distance and thus exactly the same selection function as the real data. The latter indeed is essential in order to take into account the possible systematic effects (eg. completeness, fraction of HI sources missed by the finding algorithm due

⋆ For the HI clustering see also Ryan-Weber (2006).

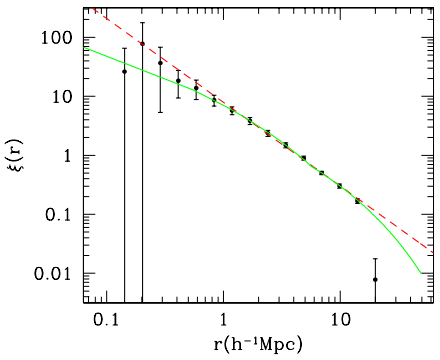

Figure 3. The spatial two-point correlation function (points) in redshift space for HIPASS sample. The error bars are estimated using the bootstrap procedure. The dashed line represent the best-fitting power low $\xi(r) = (r_0/r)^{\gamma}$ (see parameters in Table 1), while the continuous line represents the best fit ΛCDM ($\Omega_{\Lambda} = 0.7$ and $h = 0.7$) model in the framework of $b_0 = 0.63$.

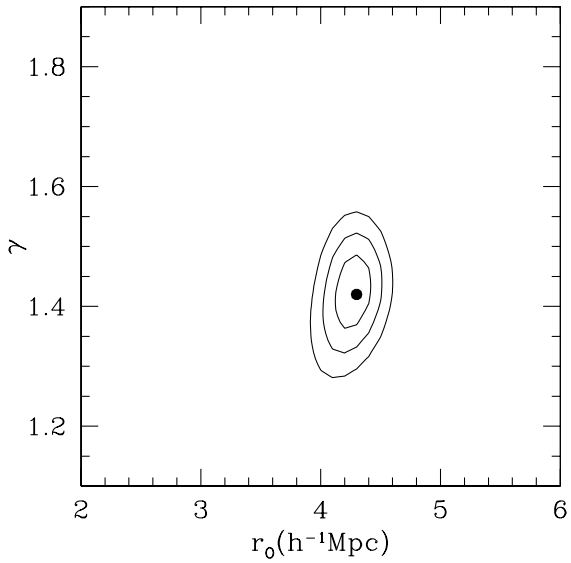

Figure 4. Iso-$\Delta\chi^2$ contours in the $r_0 - \gamma$ parameter space for the HIPASS sample. (continuous line) and S_2 (dashed line) samples. The contours correspond to 1σ ($\Delta\chi^2 = 2.30$), 2σ ($\Delta\chi^2 = 6.17$) and 3σ ($\Delta\chi^2 = 11.8$) uncertainties.

to the HIPASS flux limit). Note that we compute the errors on $\xi(r)$ from 100 bootstrap re-samplings of the data (Mo, Jing & Börner 1992).

Furthermore, we apply the correlation analysis to the HIPASS sample evaluating $\xi(r)$ in logarithmic intervals. In Fig. 3, we present the estimated two point redshift correlation function (dots); clustering is evident. We see that the correlation function below $r \geq 11h^{-1}$Mpc drops dramatically. The dashed line corresponds to the best-fitting power law model $\xi(r) = (r_0/r)^{\gamma}$, which is determined by the standard χ^2 minimisation procedure in which each correlation point is weighted by its error^{-1}. In Fig. 4 we present the iso-$\Delta\chi^2$ contours (where $\Delta\chi^2 = \chi^2 - \chi^2_{\rm min}$) in the $r_0 - \gamma$ plane. The $\chi^2_{\rm min}$ is the absolute minimum value of the χ^2. The contours correspond to 1σ ($\Delta\chi^2 = 2.30$), 2σ ($\Delta\chi^2 = 6.17$) and 3σ ($\Delta\chi^2 = 11.8$) uncertainties, respectively. The best fit parameters are listed in Table 1. Note that, the fit has been performed taking into account bins with $r \geq 0.5$ h^{-1}Mpc in order to avoid the signal from very small and therefore highly non-linear scales, while we have used no upper r cut-off (our results remain robust by varying the upper r limit within the 5 to 20 h^{-1} Mpc range).

Therefore, the clustering parameters are $r_0 = 4.3 \pm 0.3h^{-1}$Mpc and $\gamma = 1.42 \pm 0.14$. Fixing now the correlation function slope to its nominal value of $\gamma = 1.8$ we found $r_0 = 4.1^{+0.2}_{-0.3}h^{-1}$Mpc but the fit is good for $r > 1h^{-1}$Mpc. Our results is in relatively good agreement with those derived by Ryan-Weber (2006), $r_0 = 3.1 \pm 0.5h^{-1}$Mpc and $\gamma = 1.4 \pm 0.5$ using the HIPASS data. Also, in the local Universe, our results can be compared with those found by the following papers: (a) Zehavi et al. (2002) and Hawkins et al. (2003), $r_0 \simeq 5h^{-1}$Mpc and $\gamma \simeq 1.7$ for the SDSS galaxies (b) Norberg et al. (2001), $r_0 \simeq 4.9h^{-1}$Mpc and $\gamma \simeq 1.7$ for the 2dFGRS galaxies, (c) Jing, Börner & Suto (2002), $r_0 \simeq 3.7h^{-1}$Mpc and $\gamma \simeq 1.7$ using the PSCz data and finally Gonzalez-Solares et al. (2004), $r_0 \simeq 4.3h^{-1}$Mpc and $\gamma \simeq 2$ using the ELAIS sources. † However, it should point out that these authors found a somewhat greater slope for the correlation function.

3 MODEL HI SELECTED GALAXY CORRELATIONS

It is well known (cf. Kaiser 1984; Benson et al. 2000) that according to linear biasing the correlation function of the mass-tracer ($\xi_{\rm obj}$) and dark-matter one ($\xi_{\rm DM}$), are related by:

$$\xi_{\rm obj}(r) = b_0^2 \xi_{\rm DM}(r) \quad , \tag{4}$$

where b_0 is the bias factor at the present time. We quantify the underlying matter distribution clustering by presenting the spatial correlation function of the mass $\xi_{\rm DM}(r)$ [in general this is a function of redshift] as the Fourier transform of the spatial power spectrum $P(k)$:

$$\xi_{\rm DM}(r) = \frac{1}{2\pi^2} \int_0^{\infty} k^2 P(k) \frac{\sin(kr)}{kr} {\rm d}k \quad , \tag{5}$$

where k is the comoving wavenumber.

As for the power spectrum, we consider that of CDM models, where $P(k) \approx k^n T^2(k)$ with scale-invariant ($n = 1$) primeval inflationary fluctuations. We utilise the transfer function parameterisation as in Bardeen et al. (1986), with the approximate corrections given by Sugiyama's (1995) formula:

† The robustness of our results to the fitting procedure was tested using different bins (spanning from 10 to 20) and we found very similar clustering results.

Table 1. Results of the correlation function analysis for HI selected galaxies of the HIPASS sample. Errors of the fitted parameters represent 3σ uncertainties. Finally, the r_0 has units of h^{-1} Mpc.

r_0	γ	$r_0(\gamma=1.8)$	b_0	β	$K(\beta)$	$r_0^{\rm re}$	$r_0^{\rm re}(\gamma=1.8)$
4.3 ± 0.3	1.42 ± 0.14	$4.1^{+0.2}_{-0.3}$	0.63 ± 0.03	0.77	1.63	3.1 ± 0.3	$3^{+0.4}_{-0.3}$

$$T(k)=\frac{\ln(1+2.34q)}{2.34q}[1+3.89q+(16.1q)^2+$$

$$(5.46q)^3+(6.71q)^4]^{-1/4} \quad .$$

with

$$q=\frac{k}{\Omega_{\rm m}h^2{\rm exp}[-\Omega_b-(2h)^{1/2}\Omega_b/\Omega_{\rm m}]} \qquad (6)$$

where $k=2\pi/\lambda$ is the wavenumber in units of h Mpc^{-1} and Ω_b is the baryon density. Note that we also use the non-linear corrections introduced by Peacock & Dodds (1994).

In the present analysis we consider the concordance model ($\Omega_{\rm m}=0.3$) with cosmological parameters that fit the majority of observations, ie., $\Omega_{\rm m}+\Omega_\Lambda=1$, $H_0=100h$km s^{-1} Mpc^{-1} with $h\simeq0.7$ (cf. Freedman et al. 2001; Peebles and Ratra 2003; Spergel et al. 2003; Tonry et al. 2003; Riess et al. 2004; Tegmark et al. 2004; Basilakos & Plionis 2005 and references therein), baryonic density parameter $\Omega_{\rm b}h^2\simeq0.02$ (e.g. Olive, Steigman & Walker 2000; Kirkman et al 2003) and a CDM shape parameter $\Gamma=0.17$. Note that all the concordance model is normalised to have fluctuation amplitude, in a sphere of 8 h^{-1}Mpc radius, of $\sigma_8\simeq0.50(\pm0.1)\Omega_{\rm m}^{-0.53}$ (the general formula provided by Wang & Steinhardt 1998).

4 THE HIPASS BIASING

In order to quantify the HIPASS bias at the present time we perform a standard χ^2 minimisation procedure (described before) between the measured correlation function of the HIPASS sources with that expected in the concordance model

$$\chi^2(b_0)=\sum_{i=1}^{n}\left[\frac{\xi^i(r)-\xi^i_{\rm obj}(r,b_0)}{\sigma^i}\right]^2 \quad , \qquad (7)$$

where σ^i is the observed correlation function (bootstrap) uncertainty.

Doing so the bias factor at the present time is $b_0=0.63\pm0.03$. Note, that from a theoretical point of view it is well known that the bias parameter for the present day halos with $M\leq10^{12}h^{-1}M_\odot$ is $\simeq0.65$ (Sheth, Mo & Tormen 2001; Jing 1999; Seljak & Warren 2004). Thus it seems, that in the local Universe the HI selected galaxies are anti-biased tracers of the underlying matter distribution. This is to be expected, simply because our clustering analysis produces a lower corresponding correlation length (see Table 1) than the nominal one ($\sim5.5h^{-1}$Mpc). In other words, the higher or lower correlation length corresponds to a higher or lower bias at the present time respectively, being consistent with the hierarchical clustering scenario (cf. Magliocchetti et al. 2000 and references therein).

To this end, owing to the fact that the observational data are analysed in redshift space, the correlations should be amplified by the factor $K(\beta)=1+2\beta/3+\beta^2/5$ (Hamilton 1992, also see Hawkins et al. 2003) in the linear regime, where $\beta\simeq\Omega_{\rm m}^{0.6}/b_0$. Also in Table 1 we list the results of the fits for our HIPASS data, ie., the value of the HI optical bias, b_0, at the present time, as well as the redshift distortion β parameter and a measure of the $K(\beta)$ correction. Multiplying with $K^{-1}(\beta)$ to each bin of our redshift space correlation function $\xi(r)$ and repeating the fitting (see the last two columns of Table 1) the correlation length in real space is $r_0^{\rm re}=3^{+0.4}_{-0.3}h^{-1}$Mpc for $\gamma=1.42$ while using $\gamma=1.8$ we get $r_0^{\rm re}=3.1\pm0.3h^{-1}$Mpc. Finally, in Fig. 3, we plot the measured $\xi(r)$ of the HIPASS sample with the estimated (continuous line) two point correlation function for the concordance model using $b_0=0.63$. It is obvious that the fit works extremely well.

4.1 Morphological Properties

The above statistical approach (low biasing at the present epoch) introduces that there is a strong indication that the HI sources could relatively trace low density regimes of the underlying matter distribution (see also Grogin & Geller 1998). In order to investigate that, in Fig.5 we present a three dimensional view of the HIPASS data after using a novel technique which is based on the Multiscale Morphology Filters (Aragon et al. 2006 in preparation). Note that the dark and the light grey configurations correspond to filament-like structures and clusters of HI galaxies respectively. More than half of the HIPASS galaxies ($\sim55\%$) belong to morphologicaly undefined regions of the 3D distribution which are related to low density regions. This is simply to be expected because of the low biasing ($b_0\simeq0.63$). The rest of the objects are estimated to be in clusters ($\sim18\%$, light grey structures) and superclusters ($\sim27\%$, dark grey structures).

4.2 Bias Evolution

In order to understand better the effects of HI clustering, in this section we investigate the HI bias factor as a function of redshift. From a cosmological point of view, the evolution of neutral hydrogen is a powerful tool of tracing structure formation as a function of redshift because it indicates the rate of evolution of gas into stars and thus the gas consumption and the amount of the star formation in the Universe.

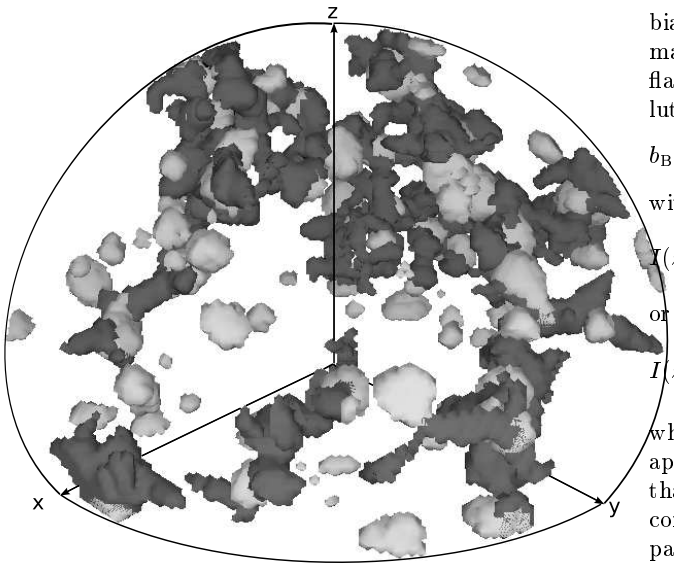

Figure 5. The 3D distribution of the HI selected galaxies in the local Universe (based on the Multiscale Morphology Filters). Note that the dark and the light grey structures correspond to superclusters and clusters of HIPASS galaxies respectively.

Over the past two decades, based on different assumptions, a number of bias evolution models have been proposed (eg. Nusser & Davis 1994; Fry 1996; Mo & White 1996; Matarrese et al. 1997; Tegmark & Peebles 1998; Basilakos & Plionis 2001). However, here we will discuss models that have been shown to describe relatively well the evolution even beyond $z \sim 1$.

- *Merging Bias Model* (hereafter B1): Mo & White (1996) have developed a model for the evolution of the the so-called correlation bias, using the Press-Schechter formalism. Utiling a similar formalism, Matarrese et al. (1997) extended the Mo & White (1996) results to include the effects of different mass scales (see also Bagla 1998). In this case the expression which describes the bias evolution is

$$b_{\rm B2}(z) = 0.41 + \frac{(b_0 - 0.41)}{D^{\beta}(z)} \quad , \tag{8}$$

with $\beta \simeq 1.8$. Note that $D(z)$ is the linear growth rate of clustering (cf. Peebles 1993) ‡ scaled to unity at the present time.

$$D(z) = \frac{5\Omega_{\rm m} E(z)}{2} \int_z^{\infty} \frac{(1+x)}{E^3(x)} {\rm d}x \quad . \tag{9}$$

with

$$E(z) = \left[\Omega_{\rm m}(1+z)^3 + \Omega_{\Lambda}\right]^{1/2} \quad . \tag{10}$$

- *Bias from Linear Perturbation Theory* (hereafter B2): Basilakos & Plionis (2001, 2003), using linear perturbation theory and the Friedmann-Lemaitre solutions of the cosmological field equations have derived analytically the functional form for the evolution of the linear bias factor, b, between the background matter and a mass-tracer fluctuation field. For the case of a spatially flat Λ cosmological model ($\Omega_{\rm m} + \Omega_{\Lambda} = 1$), the bias evolution can be written as:

$$b_{\rm B2}(z) = \mathcal{C}_1 E(z) + \mathcal{C}_2 E(z) I(z) + 1 \tag{11}$$

with

$$I(z) = \int_{1+z}^{\infty} \frac{y^3}{\left[\Omega_{\rm m} y^3 + \Omega_{\Lambda}\right]^{3/2}} {\rm d}y \tag{12}$$

or

$$I(z) = (1+z)^{-1/2} F\left[\frac{1}{6}, \frac{3}{2}, \frac{7}{6}, -\frac{\Omega_{\Lambda}}{\Omega_{\rm m}(1+z)^3}\right] \tag{13}$$

where F is the hyper-geometric function. Note that this approach gives a family of bias curves, due to the fact that it has two unknown parameters, (the integration constants $\mathcal{C}_1, \mathcal{C}_2$). Basilakos & Plionis (2001, 2003) compared the B2 bias evolution model with other models as well as with the HDF (Hubble Deep Field) biasing results (Arnouts et al. 2002), and found a very good consistency. Of course in order to obtain partial solutions for $b(z)$ we need to estimate the values of the constants $\mathcal{C}_1$ and $\mathcal{C}_2$), which means that we need to calibrate the $b(z)$ relation using two different epochs: $b(0) = b_0$ and $b(z_1) = b_1$.

Therefore, utilised the general bias solution (see eq.11), it is routine to obtain the expressions for the above constants as a function of b_0 and b_1:

$$\mathcal{C}_1 = \frac{(b_0 - 1)E(z_1)I(z_1) - (b_1 - 1)E(0)I(0)}{E(0)E(z_1)[I(z_1) - I(0)]} \tag{14}$$

$$\mathcal{C}_2 = \frac{E(0)(b_1 - 1) - E(z_1)(b_0 - 1)}{E(0)E(z_1)[I(z_1) - I(0)]} \quad , \tag{15}$$

where for the present epoch we have: $b_0 \simeq 0.63$, $E(0) = 1$ and $I(0) \simeq 9.567$. In the distant Universe we calibrate the B2-model by using Cooke et al. (2006) value of the bias for Damped Lyman-a systems (hereafter DLA; see solid point in Fig.6) which gives, $b(3) \simeq 2.4$ §. The DLA systems are quasar absorbers along the line-of-sight at high redshifts and they are classified according to their large column densities, $N_{\rm HI} \geq 2 \times 10^{20}$atom cm^{-}2 (see Wolfe et al. 1986; Peroux et al. 2001). These systems play a vital role in the hierarchy of the structure formation because the large column densities can protect large amounts of neutral gas from the background ionizing (Zwaan & Prochaska 2006) and thus they produce an ideal environment for star formation.

Having known the bias factor at the present time in Fig.6 we plot the quantity $b(z)$ as a function of redshift for the concordance cosmological model and for different bias evolution models (B1 continuous line and B2 dashed line). It is quite obvious that the behaviour of the function $b(z)$ characterises the tracing evolution with epoch; in particular at low redshifts ($z \leq 0.9$) we have a sort of anti-bias picture but latter on owing to the fact that the bias is a monotonically increasing function of redshift for both B1 and B2 biasing models the HI

‡ $D(z) = (1+z)^{-1}$ for an Einstein-de Sitter Universe.

§ For $z = 3$ we get $E(3) \simeq 4.61$ and $I(3) \simeq 6.039$

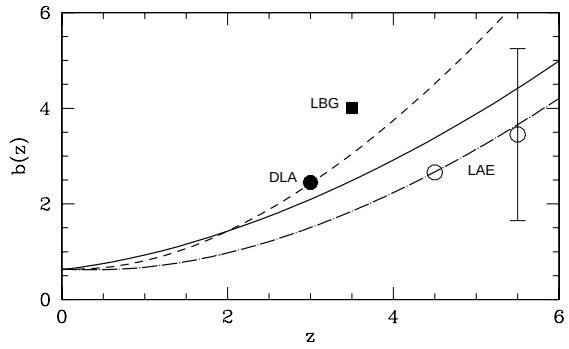

Figure 6. The bias factor as a function of redshift for the B1 (continuous line) and B2 (dashed line) bias model respectively. Different point types represent different values of bias. The solid circle represents the observational bias for the Damped Lyman-a systems (DLA) of Cooke et al. (2006). The square like symbol corresponds to Lyman break galaxies (LBG, Steidel et al. 1998) while the open circle represents the bias for the Lyman-a emitters (LAE) derived by Ouchi et al. (2005) and Kovač et al. (in preparation). Note that the dot-dashed line represents the bias behavior for the LAE galaxies.

sources are biased with respect to the underlying matter distribution. Also up to redshift 2.2 both models give almost the same predictions. However, at very high redshifts Fig.6 clearly shows that the bias of those neutral hydrogen sources behaves different in the different biasing models.

We further compare our analytic solutions with observations provided by (a) Steidel et al. (1998) which confirmed that the Lyman-break galaxies (hereafter LBG; see solid square in Fig.6) are very strongly biased tracers of mass (see also Adelberger et al. 1998; Kashikawa et al. 2006) and they found that $b(3.4) \simeq 4$ and (b) Ouchi et al. (2005) utilising Lyman-a emitters found $b(5.7) \simeq 3.8 \pm 1.8$ while Kovač et al (in preparation) found $b(4.5) = 2.6$ (hereafter LAE; see open circle in Fig.6). In that case, we compare in Fig.6 (dot dashed line) the B2-model, evaluated at $z = 4.5$ [¶] using the LAE results (Kovač et al. in preparation). It is quite evident that our model fits better the z-dependance of the observational LAE galaxy bias. Our strong biasing predictions are also in agreement with those found from simulations of galaxy formation (Kauffmann et al. 1999) which means that such strong biasing at large redshifts can be justified if structures are formed at the highest rare peaks of matter density (Mo & White 2002). From the observational point of view the last few years many authors using Lyman-a systems have found high overdensities ($\delta > 50$) at high redshifts. Indeed, Steidel et al. (1998) using LBGs found a very high overdensity peak (protocluster) at $z = 3.1$. Recently, Venemans et al. (2004), Miley et al. (2004) and Ouchi et al. (2005) found protoclusters of LAE galaxies at high redshifts ($z \geq 4$). Also cross correlation analysis has shown (Cooke et al. 2006) that the LBGs associated with the DLA systems at the same redshift a fact which implies that perhaps the LBGs are in the same parent system that contains DLAs (Cooke et al. 2005).

[¶] For $z = 4.5$ we get $E(4.5) \simeq 7.11$ and $I(4.5) \simeq 5.175$

5 CONCLUSIONS

We have studied the clustering properties of the HI 21-cm emission line sources from HIPASS catalogue in redshift space. We find that if the two point cluster correlation function is modelled as a power law, $\xi(r) = (r_0/r)^{\gamma}$, then the best-fitting parameters are $r_0 = 4.3 \pm 0.3h^{-1}$ Mpc with $\gamma = 1.42 \pm 0.14$. Fixing the slope to its universal value $\gamma = 1.8$, we obtain $r_0 = 4.1^{+0.2}_{-0.3}h^{-1}$Mpc.

Comparing the measured spatial correlation function for the HI selected galaxies with the theoretical predictions of the preferred ΛCDM cosmological model ($\Omega_{\rm m} = 1 - \Omega_{\Lambda} = 0.3$) and two different bias evolution models, we find that the present bias value is $b_0 \simeq 0.63$, suggesting that the HI selected galaxies could potentially trace the low density regimes in the local Universe in agreement with previous studies (Grogin & Geller 1998). Also, we investigate the evolution of the linear bias factor, $b(z)$, and we find that the anti-bias behaviour extends up to $z \leq 0.9$. Our predictions are consistent with the observational bias results of the Lyman-a galaxies. Furthermore, we estimate the HIPASS redshift space distortion parameter $\beta \simeq 0.77$ and we conclude that the amplitude of the HI redshift correlation function increases by a factor of 1.63. Therefore, taking into account this correction the HI correlation length in real space is $r_0^{\rm re} = 3^{+0.4}_{-0.3}h^{-1}$Mpc for $\gamma = 1.42$ while using $\gamma = 1.8$ we get $r_0^{\rm re} = 3.1 \pm 0.3h^{-1}$Mpc.

ACKNOWLEDGEMENTS

SB acknowledges support by the Nederlandse Onderzoekschool voor Astronomie (NOVA) grant No 366243.

REFERENCES

Adelberger, K. L., Steidel, C. C., Giavalisko, M., Dickinson M., Pettini, M., &, Kellogg, M., 1998, ApJ, 505, 18
Arnouts, S., et al.., 2002, MNRAS, 329, 355
Bagla, J. S., 1998, MNRAS, 299, 424
Barnes et al., 2001, MNRAS, 322, 486
Bardeen, J.M., Bond, J.R., Kaiser, N. & Szalay, A.S., 1986, ApJ, 304, 15
Basilakos, S. & Plionis, M., 2001, ApJ, 550, 522
Basilakos, S. & Plionis, M., 2003, ApJ, 593, L61
Basilakos, S. & Plionis, M., 2005, MNRAS, 360, L35
Benson A. J., Cole S., Frenk S. C., Baugh M. C., & Lacey G. C., 2000, MNRAS, 311, 793
Colless, M., et al., 2001, MNRAS, 328, 1039
Cooke, J. W., Wolfe, A. M., Prochaska, J. X.,&, Gawiser, E., 2005, ApJ, 621, 596
Cooke, J. W., Wolfe, A. M., Gawiser, E., &, Prochaska, J. X., 2006, ApJ, 636, L9
Doyle, M. T., et al., 2005, MNRAS, 361, 34

Freedman, W., L., et al., 2001, ApJ, 553, 47
Fry J.N., 1996, ApJ, 461, 65
Gonzalez-Solares, E. A., et al., MNRAS, 352, 44
Grogin, N. A., &, Geller, M. J., 1998, ApJ, 505, 506
Jing, Y. P., 1999, ApJ, 515, 45
Jing, Y. P., Börner, G & Suto, Y., 2002, ApJ, 564, 15
Hamilton, A. J. S., 1992, ApJ, 385, L5
Hamilton, A. J. S., 1993, ApJ, 417, 19
Hawkins, Ed, et al., 2003, MNRAS, 346, 78
Kaiser N., 1984, ApJ, 284, L9
Kashikawa, N., et al., 2006, ApJ, 637, 631
Kauffmann G., Golberg, J. M., Diaferio A., &, White S. D. M., 1999, MNRAS, 307, 529
Kirkman, D., Tytler, D., Suzuki, N., O'Meara, J.M. & Lubin, D., 2003, ApJS, 149, 1
Magliocchetti, M., Bagla, J. S., Maddox, S. J. & Lahav, O., 2000, MNRAS, 314,546
Mataresse, S., Coles, P., Lucchin, F. & Moscardini, L., 1997, MNRAS, 286, 115
Meyer, G. R., et al., 2004, MNRAS, 350, 1195
Miley, G. K.., et al., 2004, Nature, 427, 47
Mo, H. J., Jing, Y. P. & Börner, G., 1992, ApJ, 392, 452
Mo, H.J, & White, S.D.M 1996, MNRAS, 282, 347
Mo, H.J, & White, S.D.M 2002, MNRAS, 336, 112
Norberg, P., et al., 2001, MNRAS, 328, 64
Nusser, M., & Davis, M., 1994, ApJ, 421, L1
Olive, K.A., Steigman, G. & Walker, T.P., 2000, Phys.Rep., 333, 389
Oliver, S., et al., 2000, MNRAS, 316, 749
Ouchi, M., et al., 2005, ApJ, 620, l10
Peacock, A. J., &, Dodds, S. J., 1994, MNRAS, 267, 1020
Peebles P.J.E., 1993, Principles of Physical Cosmology, Princeton University Press, Princeton New Jersey
Peebles P.J.E., &, Ratra, B., 2003, RvMP, 75, 559
Peroux, C., Storrie-Lombardi, L. J., McMahon, R. G., Irwin, M., &, Hook, I. M., 2001, AJ, 121, 1799
Riess, A. G., et al., 2004, ApJ, 607, 665
Ryan-Weber, E. V., MNRAS, 2006, in press, *astro-ph/0601055*
Saunders, W., et al., 2000, MNRAS, 317, 55
Seljak U., &, Warren, M. S., 2004, MNRAS, 355, 129
Sheth R. K., Mo H. J., &, Tormen, G., 2001, MNRAS, 323, 1
Spergel, D. N., et al., 2003, ApJs, 148, 175
Steidel C.C., Adelberger L.K., Dickinson M., Giavalisko M., Pettini M., &, Kellogg M., 1998, ApJ, 492, 428
Sugiyama, N., 1995, ApJS, 100, 281
Tegmark M. & Peebles P.J.E, 1998, ApJL, 500, L79
Tegmark M., et al., 2004, Phys. Rev. D., 69, 3501
Tonry, et al. , 2003, ApJ, 594, 1
Wang, L. & Steinhardt, P.J., 1998, ApJ, 508, 483
Wolfe, A. M., Tumshek, D. A., Smith, H. E., &, Cohen, R. D., 1986, ApJS, 61, 249
Venemans, B. P., et al., 2004, A&A, 427, L17
York, D. G., 2000, AJ, 120, 1579
Zehavi I., et al., 2002, ApJ, 571, 172
Zwaan, M. A., et al., 2004, MNRAS, 350, 1210
Zwaan, M. A., Meyer, M. J., Staveley-Smith, L., Webster, R. L., 2005, MNRAS, 359, L30
Zwaan, M. A., &, Prochaska, J. X., 2006, ApJ, in press, *astro-ph/0601655*